https://ntrs.nasa.gov/search.jsp?R=20030038812 2018-05-15T15:53:52+00:00Z

NASA/CR—2003-212202

CCL–02–003



Subgrid Combustion Modeling for the Next Generation National Combustion Code

Suresh Menon, Vaidyanathan Sankaran, and Christopher Stone
Georgia Institute of Technology, Atlanta, Georgia

April 2003

The NASA STI Program Office . . . in Profile

Since its founding, NASA has been dedicated to the advancement of aeronautics and space science. The NASA Scientific and Technical Information (STI) Program Office plays a key part in helping NASA maintain this important role.

The NASA STI Program Office is operated by Langley Research Center, the Lead Center for NASA's scientific and technical information. The NASA STI Program Office provides access to the NASA STI Database, the largest collection of aeronautical and space science STI in the world. The Program Office is also NASA's institutional mechanism for disseminating the results of its research and development activities. These results are published by NASA in the NASA STI Report Series, which includes the following report types:

- TECHNICAL PUBLICATION. Reports of completed research or a major significant phase of research that present the results of NASA programs and include extensive data or theoretical analysis. Includes compilations of significant scientific and technical data and information deemed to be of continuing reference value. NASA's counterpart of peer-reviewed formal professional papers but has less stringent limitations on manuscript length and extent of graphic presentations.

- TECHNICAL MEMORANDUM. Scientific and technical findings that are preliminary or of specialized interest, e.g., quick release reports, working papers, and bibliographies that contain minimal annotation. Does not contain extensive analysis.

- CONTRACTOR REPORT. Scientific and technical findings by NASA-sponsored contractors and grantees.

- CONFERENCE PUBLICATION. Collected papers from scientific and technical conferences, symposia, seminars, or other meetings sponsored or cosponsored by NASA.

- SPECIAL PUBLICATION. Scientific, technical, or historical information from NASA programs, projects, and missions, often concerned with subjects having substantial public interest.

- TECHNICAL TRANSLATION. English-language translations of foreign scientific and technical material pertinent to NASA's mission.

Specialized services that complement the STI Program Office's diverse offerings include creating custom thesauri, building customized databases, organizing and publishing research results . . . even providing videos.

For more information about the NASA STI Program Office, see the following:

- Access the NASA STI Program Home Page at ***http://www.sti.nasa.gov***

- E-mail your question via the Internet to help@sti.nasa.gov

- Fax your question to the NASA Access Help Desk at 301–621–0134

- Telephone the NASA Access Help Desk at 301–621–0390

- Write to:
  NASA Access Help Desk
  NASA Center for AeroSpace Information
  7121 Standard Drive
  Hanover, MD 21076

NASA/CR—2003-212202

CCL–02–003



Subgrid Combustion Modeling for the Next Generation National Combustion Code

Suresh Menon, Vaidyanathan Sankaran, and Christopher Stone
Georgia Institute of Technology, Atlanta, Georgia

Prepared under Grant NAG3–2660

National Aeronautics and
Space Administration

Glenn Research Center

April 2003

The Propulsion and Power Program at
NASA Glenn Research Center sponsored this work.

Available from

NASA Center for Aerospace Information
7121 Standard Drive
Hanover, MD 21076

National Technical Information Service
5285 Port Royal Road
Springfield, VA 22100

Available electronically at http://gltrs.grc.nasa.gov

Subgrid Combustion Modeling for the *Next Generation* National Combustion Code

Suresh Menon, Vaidyanathan Sankaran, and Christopher Stone
School of Aerospace Engineering
Georgia Institute of Technology
Atlanta, Georgia 30332

1. Introduction

Recent more stringent emission regulations have pushed for the development of more fuel-efficient and low-emission combustion systems for both ground-based and flight gas turbine applications. Experimental estimate of pollutant formation is limited due to the inability to probe non-intrusively, the highly three-dimensional flame zone. As a result, detailed understanding of where (and why) the pollutants (primarily, NOx, CO and unburned hydrocarbons, including soot) are forming is difficult, if not impossible to determine using experimental data. This is a major stumbling block in the design of the next generation, fuel-efficient gas turbine engines. Numerical prediction could help but most codes currently in use employ steady state methods and are unable to capture the unsteady dynamics that control the pollutant formation process. In addition to the inaccuracy in the prediction of NOx formation, CO emission is also not predicted very well under dynamic conditions. For example, recent studies (Bhargava, 2000) have shown that as the equivalence ratio is reduced, CO emission first decreases and then suddenly increases rapidly. This sudden increase occurs during lean combustion when perturbation to the flame can cause instability and also lead to incomplete combustion. The condition at which this sudden increase occurs is very important to predict and control since it impacts the performance and efficiency of the gas turbine engine. However, so far, no numerical simulation tool has been able to predict this behavior.

Accurate prediction of unsteady combustion requires a comprehensive model that can predict flame structure and propagation characteristics, pollutant formation and transport, and ignition/extinction phenomena over a wide range of flow conditions in high Reynolds (Re) number, three-dimensional (3D) flows as in a gas turbine combustor. Direct Numerical Simulations (DNS) are not practical since the resolution and computational resource requirements far exceed the present and even future capability. A simulation approach that has become popular in recent years is large-eddy simulation (LES). In LES, all scales larger than the grid resolution are numerically simulated using a space- and time-accurate scheme while the effect of scales below the grid resolution is modeled using a subgrid model. Although many LES studies have been reported, a validated LES approach for practical systems is yet to be demonstrated although the approaches discussed in this paper have shown a serious potential to achieve this capability.

Over the last few years, there has been a major effort at NASA-GRC to develop a unique computational capability called the Numerical Propulsion Simulation System (NPSS). In this approach, a simulation model that will allow simultaneous calculation of the flow in the entire engine (i.e., inlet, compressor, combustor, turbine and nozzle) is currently being pursued and developed. Within this structure, the simulation tool for the combustor, called the National Combustion Code (NCC) has reached a major state of maturity and is currently being evaluated for practical applications both at NASA and at industrial R&D sites (e.g., GEAEC). Various advanced models have been implemented to make NCC a state-of-the-art modeling tool and its application to various problems are being demonstrated and/or discussed in numerous recent papers (e.g., Liu, 2001, Raju, 2001, Lannetti et al., 2001, Moder, 2001, Ajmani, 2001, Shih et al., 2001).

The NCC is based on Reynolds-Averaged Navier-Stokes (RANS) modeling approach and is the current choice since it is computationally efficient when complex systems have to be simulated. However, it has some inherent (and well-known) limitations. In RANS modeling, the effect of all turbulent length and time scales are modeled using global turbulence models such as the popular k-e model. Closure of the turbulent reaction rate and turbulent species flux are also based on global model that ignore some fundamental physics of turbulent mixing and combustion. For example, the dynamical interactions between flow, unsteady heat release, acoustic (pressure) oscillation and turbulence is lost since only the time-averaged flow field can be simulated with such an approach. These very important phenomena directly impact fuel-air mixing process and are controlled by processes that occur at the small-scales. Unfortunately, even unsteady RANS models cannot resolve these fine-scale interactions in a physically consistent manner since all these effects are modeled.

In this three-year research study, we plan to take advantage of two crucial developments: (a) the demonstrated capability of NCC to simulate flows in complex configurations using robust algorithms and (b) the recent demonstration of a unique subgrid combustion model for LES applications. We (the team from Georgia Tech and NASA/GRC) will combine these two capabilities into a new simulation model, denoted hereafter NCCLES that will contain all the capabilities of the original NCC but will now contain additional algorithms that will allow it to be used in a LES mode. It is envisioned that NCCLES will eventually become a specialized tool that will address issues that the original NCC cannot.

2. Technical Objectives

The proposed research is carrying out both model development and model implementation simultaneously. The model development effort (which will primarily be at Georgia Tech) is addressing issues related to complex high-Re flows, including supersonic flows. Model implementation of the subgrid kinetic energy model and the subgrid mixing and combustion model within NCC is being carried out at NASA/GRC. Substantial progress in both the collaborative effort and in the new advances in the LES subgrid models has been achieved already. More details of the progress made to date are summarized below.

The overall technical objectives of this three-year project are:

1. ***Collaborate with the NCC team and provide algorithms that will allow them to convert the current NCC algorithm to a LES version.***

   It is worth noting that since many of the baseline algorithms are already developed, transition of this technology to the NCC team has already begun. More details of the current collaborative effort are summarized below.

2. ***Further develop the subgrid models for momentum and scalar transport for implementation into NCCLES.***

   This is a major effort since NCCLES is expected to deal with many different scenarios and the subgrid models have to be able to simulate all such flows without compromising the physics. Therefore, the models currently operational need to be re-evaluated in this context. This effort has already begun and we have made substantial progress to-date.

3. ***Collaborate with the NCC team to demonstrate and validate the next generation NCC for LES applications.***

   All the models developed during this research will be implemented in our in-house code, LESLIE3D that has been extensively used for such studies. Once the validation of the new algorithms is completed, we will transition this technology in a timely manner to the NCCLES for further evaluation. Close collaboration with the NCC team will be maintained during this effort.

3. The LESLIE3D Code

The LESLIE3D code is a fully compressible, 3D finite volume solver that has been used extensively in the past to carry out LES studies of complex turbulent reacting flows as in the gas turbine combustor. The code can be used for both DNS and LES and is second-order accurate in time and has an option to do either second or fourth-order accurate scheme in space. A constant coefficient model and a localized dynamic subgrid model (where the model coefficients are obtained as a part of the simulation and hence, in this case, the closure has no parameters to set or adjust) for the subgrid kinetic energy are options in the code. In addition, models for subgrid combustion are also implemented for both premixed and non-premixed combustion. For completeness, the LES model equations and closures are summarized here.

3.1 The LES Equations

The compressible LES equations are obtained by spatial filtering of the conservation equations of mass, motion, energy and species. The final set of LES equations are:

$$
\begin{aligned}
&\frac{\partial \overline{\rho}}{\partial t}+\frac{\partial \overline{\rho}\widetilde{u}_i}{\partial x_i}=0\\
&\frac{\partial \overline{\rho}\widetilde{u}_i}{\partial t}+\frac{\partial}{\partial x_j}\left[\overline{\rho}\widetilde{u}_i\widetilde{u}_j+\overline{p}\delta_{ij}-\overline{\tau}_{ij}+\tau_{ij}^{sgs}\right]=0\\
&\frac{\partial \overline{\rho}\widetilde{E}}{\partial t}+\frac{\partial}{\partial x_i}\left[\left(\overline{\rho}\widetilde{E}+\overline{p}\right)\widetilde{u}_i+\overline{q}_i-\widetilde{u}_j\overline{\tau}_{ij}+H_i^{sgs}+\sigma_{ij}^{sgs}\right]=0\\
&\frac{\partial \overline{\rho}\widetilde{Y}_m}{\partial t}+\frac{\partial}{\partial x_i}\left[\overline{\rho}\widetilde{Y}_m\widetilde{u}_i-\overline{\rho}D_m\frac{\partial \widetilde{Y}_m}{\partial x_i}+\Phi_{i,m}^{sgs}+\Theta_{i,m}^{sgs}\right]=\overline{\dot{w}_m}
\end{aligned}
\tag{1}
$$

Here, the filtered total specific energy $\widetilde{E}$ is given by: $\widetilde{E}=\widetilde{e}+\frac{\widetilde{u}_l\widetilde{u}_l}{2}+k^{sgs}$, where k^{sgs} is the subgrid turbulent kinetic energy given by $k^{sgs}=\left(u_lu_l-\widetilde{u}_l\widetilde{u}_l\right)/2$. The unclosed terms $\tau_{ij}^{sgs},H_i^{sgs},\sigma_{ij}^{sgs},\Phi_{i,m}^{sgs},\Theta_{i,m}^{sgs}$ represent the subgrid stress tensor, heat flux, viscous work, species mass flux and species diffusive mass flux, respectively, and are:

$$
\begin{aligned}
\tau_{ij}^{sgs}&=\overline{\rho}\left(u_iu_j-\widetilde{u}_i\widetilde{u}_j\right)\\
H_{ij}^{sgs}&=\overline{\rho}\left(H_Tu_j-H_T\widetilde{u}_j\right)\\
\sigma_j^{sgs}&=\overline{\rho}\left(\overline{u_i\tau_{ji}}-u_i\overline{\tau}_{ji}\right)\\
\Phi_{k,j}^{sgs}&=\overline{\rho}\left(Y_ku_j-\widetilde{Y}_k\widetilde{u}_j\right)\\
\Theta_{k,j}^{sgs}&=\overline{\rho}\left(Y_kU_{k,j}-\widetilde{Y}_k\widetilde{U}_{k,j}\right)
\end{aligned}
\tag{2}
$$

The pressure $\overline{p}$ is obtained from the equation of state for a thermally perfect gas, $p=\overline{\rho}RT$. The mixture gas constant is given by $R=\sum_m Y_mR_m$. A similar expression also applies for mixture specific heats C_p and C_v where $C_p-C_v=R$.

3.2 Subgrid Closure for Convective Fluxes

Closure of the subgrid flux terms is achieved using a transport equation for the subgrid kinetic energy per unit mass $k^{sgs}=\frac{1}{2}\left[\left(\widetilde{u_k^2}\right)-\widetilde{u}_k^2\right]$ (Menon et al., 1996):

$$
\frac{\partial \overline{\rho}k^{sgs}}{\partial t}+\frac{\partial}{\partial x_i}\left(\overline{\rho}\widetilde{u}_ik^{sgs}\right)=P^{sgs}-D^{sgs}+\frac{\partial}{\partial x_i}\left(\overline{\rho}\frac{\nu_t}{\mathrm{Pr}_t}\frac{\partial k^{sgs}}{\partial x_i}\right)
\tag{3}
$$

Here, $P^{sgs}=-\tau_{ij}^{sgs}\frac{\partial \widetilde{u}_i}{\partial x_j}$ and $D^{sgs}=C_\varepsilon\overline{\rho}\left(k^{sgs}\right)^{3/2}/\overline{\Delta}$ are the production and dissipation terms, respectively. Subgrid stress tensor is closed by an eddy viscosity hypothesis based on the subgrid kinetic energy. Thus, $\tau_{ij}^{sgs}=-2\overline{\rho}\nu_t\left(\widetilde{S}_{ij}-\frac{1}{3}\widetilde{S}_{kk}\delta_{ij}\right)+\frac{2}{3}\overline{\rho}k^{sgs}\delta_{ij}$ where the eddy viscosity is $\nu_t=C_\nu\left(k^{sgs}\right)^{1/2}\overline{\Delta}$.

The two model coefficients, C_ν and C_ε, are 0.067 and 0.916, respectively for the constant coefficient model based on earlier studies (Chakravarthy and Menon, 2001a, 2001b). A localized dynamic approach developed using a scale-similarity approach can also be used to obtain these coefficients model dynamically (Kim and Menon, 1999, Kim et al., 1999, Kim and Menon, 2000). Given the subgrid kinetic energy, the unclosed terms in LES equations can be modeled. For example, the sub-grid heat flux and the subgrid mass flux are:

$$H_i^{sgs} = -\overline{\rho}\frac{\nu_t}{\mathrm{Pr}_t}\frac{\partial \widetilde{h}}{\partial x_i}$$

$$\Phi_{i,m}^{sgs} = -\overline{\rho}\frac{\nu_t}{Sc_t}\frac{\partial \widetilde{Y}_m}{\partial x_i}$$

Where $\boldsymbol{Sc_t}$ and $\mathbf{Pr}_t$ are the turbulent Schmidt number and Prandtl number. At present, these are assumed to be unity.

LESLIE3D contains closure models for both premixed and non-premixed mixing and combustion process. These are briefly summarized below.

3.3 Subgrid Flame Speed Model

This approach is only applicable to premixed combustion in the flamelet regime. In this case, the flame is much thinner than the smallest scales of turbulence and therefore, turbulence can only wrinkle the flame but cannot affect the flame structure. Flame wrinkling and stretching increases the effective flame surface area and therefore, can increase the burning velocity. In the flamelet limit, a simplification can be carried out whereby the flame is modeled as an infinitely thin surface that separates the unburnt reactants from the burned products. In this approach, reaction kinetics need not be solved and the problem essentially reduces to the tracking of the flame front. This approach has been used quite successfully to simulate lean premixed combustion in full-scale gas turbine engine such as the General Electric LM6000. We will be using this version of the LESLIE3D initially to develop and evaluate the NCCLES.

The model involves the transport solution of a progress variable G that lies in the range [0,1] with the flame located between the two limits. The G-field is convected by the flow field and also propagated normal to itself with the normal burning velocity. In the laminar case, this is the classical laminar burning velocity (which contains all the thermo-chemical effects of finite-rate kinetics) but in the turbulent field, a closure is needed to estimate the effective turbulent burning speed. The LES model for the flame front is obtained by the solution of the following filtered G-equation:

$$\frac{\partial \overline{\rho}\widetilde{G}}{\partial t} + \frac{\partial \overline{\rho}\widetilde{u}_i\widetilde{G}}{\partial x_i} = -S^{sgs} - \frac{\partial}{\partial x_i}\overline{\rho}(u_i G - \widetilde{u}_i\widetilde{G}) \tag{4}$$

Here, the terms of the right-hand-side require closure. Here, S^{sgs} is the turbulent flame propagation term typically given as: $S^{sgs} = S_T\left|\nabla\widetilde{G}\right|$ where $S_T = S_T(u', S_L)$ is the turbulent flame speed that is modeled in terms of the laminar flame speed and the subgrid turbulence (obtained from subgrid kinetic energy: $k^{sgs} = \frac{1}{2}\left[\left(\widetilde{u_k^2}\right) - \widetilde{u}_k^2\right]$). In the present study, a model proposed by Pocheau has been used to obtain the turbulent burning velocity. The second term $G_i^{sgs} = (u_i G - \widetilde{u}_i\widetilde{G})$ is the subgrid convective flux that also requires closure. Various models have been proposed for this term: (a) localized dynamic eddy diffusion model (Kim and Menon, 2000), (b) flame curvature model (Peters, 2000), etc. We have evaluated all these models as reported below.

Heat release is incorporated by including the heat of formation in the definition of the internal energy using the following relationship: $e = C_v\widetilde{T} + e_f H(\widetilde{G} - G_0)$ where, H(Q) is the Heavy-side function and G_0 is an arbitrarily chosen value in the range [0,1] where the flame is located. More details are given elsewhere (Kim et al., 1999, Kim and Menon, 2000) and therefore, avoided here, for brevity. Although this approach is computationally very efficient (since species equations and/or finite-rate kinetics do not have to be modeled), this approach cannot be used to capture species variations and/or be used to predict pollutant formation. To do this, one has to resort to the more complex finite-rate kinetics closure.

3.4 Subgrid Scalar Closure using Eddy Diffusivity

For both premixed and non-premixed combustion, if detailed kinetics is of interest multi-species equations have to be solved along with the LES equations. In this case, two terms, the sub-grid scalar flux, $\theta_{i,m}^{sgs} = \overline{\rho}[\widetilde{V_{i,m}Y_m} - \widetilde{V}_{i,m}\widetilde{Y}_m]$ and the filtered reaction rate term, $\overline{\dot{\omega}}_m$ require closure. In a conventional approach, a subgrid gradient approximation: $\theta_{i,m}^{sgs} \approx -\frac{\overline{\rho}\nu_t\nabla\widetilde{Y}_m}{Sc_m}$ where Sc_m is a turbulent Schmidt number, is employed for the subgrid scalar flux. Note that, since large-scale motion is resolved in a LES, associated counter-gradient processes are resolved (even when a gradient closure is employed for $\theta_{i,m}^{sgs}$). The closure for $\overline{\dot{\omega}}_m$ s complicated due to its highly non-linear nature. Assumed PDF subgrid models, subgrid Eddy Breakup and subgrid Eddy Dissipation models, all of which are variants of the models used in RANS codes, have been proposed for this closure.

However, at this time, the accurate closures for the reaction rate within the conventional LES context have yet to be established. In order to ensure accuracy, we have developed a new closure model based on a subgrid simulation approach. This is described in the next section.

3.5 Subgrid Scalar Closure using LEM

In the LEM closure, the species fields evolve within each LES cell due to localized, stochastic reaction-diffusion processes, and are then transported across the LES cells due to convective flux. The local sub-grid domain within each LES cell is resolved on a one-dimensional domain that resolves all scales of motion and thus, processes within this domain can be considered a localized 1-D Direct Numerical Simulation. Thus, all scales down to the Kolmogorov and Batchelor's scale are resolved in this simulation (Menon et al., 1993, Calhoon and Menon, 1996, Chakravarthy and Menon, 2001a, 2001b).

To describe this method, consider an "exact" reaction-diffusion equation for a scalar ϕ:

$$\frac{\partial \phi}{\partial t} + (\tilde{u}_i + u_i{}') \frac{\partial \phi}{\partial x_i} = \frac{\partial}{\partial x_i}[D_\phi \frac{\partial \phi}{\partial x}] + \dot{\omega}_\phi \tag{5}$$

Here, $\tilde{u}_i$ and u_i' are the resolved and unresolved velocities, respectively. Also, u_i' is due to both the Lagrangian convection through the cell face u'_{lag}, and turbulent convection at scales smaller than the resolved grid, u'_{stir}

The one dimensional linear-eddy domain, in every LES cell is initialized with a constant number of LEM cells. The number of linear-eddy cells that are needed to resolve all the sub-grid scales is computed based on a subgrid Reynolds number probability density, obtained over the whole of the computational domain. The length of the linear eddy domain is set equal to the LES filter width. Since the Lagrangian convection across the LES cell face is based on the mass, the volume of the linear-eddy cell is also carried as an additional scalar. At the start of the simulation, volume of each linear eddy cell is set to have an equal fraction of the LES cell volume. At each LES step, after updating the density, momentum and the energy field, LEM is used to evolve the scalar field. Note that, as opposed to the conventional scalar closure approach described in the previous section, no scalar equations are solved on the resolved grid.

Using a fractional splitting technique, we can split the equation (5) as follows:

Subgrid Processes:
$$\int_{t_o}^{t+\Delta t_{LES}} [u'_{stir} \frac{\partial \phi}{\partial x_i} + \frac{\partial}{\partial x_i}[D_\phi \frac{\partial \phi}{\partial x}] + \dot{\omega}_\phi] dt \tag{6}$$

Supergrid Convection:
$$\frac{\phi^* - \phi^n}{\Delta t_{LES}} = (\tilde{u}_i + u'_{lag}) \frac{\partial \phi}{\partial x_i} \tag{7}$$

Equation (6) represents the sub-grid reaction-diffusion processes that occur locally within each LES cell using the LEM model. Three processes occur within each LES cell: (a) turbulent convection at scales smaller than the resolved grid (which is modeled using stochastic stirring events called triplet maps, (b) molecular diffusion and finite-rate kinetics, and (c) volumetric heat release. Additional details are given in cited

references. After the first two subgrid processes, volumetric gas expansion caused by heat release is implemented by expanding each linear-eddy cell in the domain by an amount equal to $\Delta V_{LEM,i}^{n+1} = \frac{\rho_i^n}{\rho_i^{n+1}}$.

Equation (7), which represents the advection (convective transport) of the scalar field by the resolved velocity field is modeled by a volume of fluid (VOF) approach (Chakravarthy and Menon, 2001a, 2001b) in which the linear eddy cells are convected across LES cell face at the advective time scale given by $\Delta t_{conv} = (CFL)\min \frac{\Delta x_{LES}}{(u_i + u'_{sgs})}$. Ideally, splicing in a compressible simulation can be performed every Δt_{conv} step. But, in order to provide a close coupling between the fluid dynamic and the flame front evolution, splicing is performed every LES time step. This considerably improves the numerical stability of the simulation.

On a general three-dimensional grid the mass transfer from any control volume to any neighboring control volume is also predominantly 3D. As a result, different numbers of linear-eddy cells are transported in different spatial directions. In the numerical implementation of the scalar advection, the 3D advection operator is approximated by a sequence of three, one dimensional advection operators. So the order in which these operators act on the scalar field can have a significant effect on the scalar field evolution. In the new algorithm, the linear-eddy cells going out in the direction of largest out-flux are fluxed out first from the right end of the sub-grid domain. Similarly the largest influx is added first to the left end of linear eddy domain. This upwind type flux update has been used successfully in the past (Chakravarthy and Menon, 2001a, 2001b).

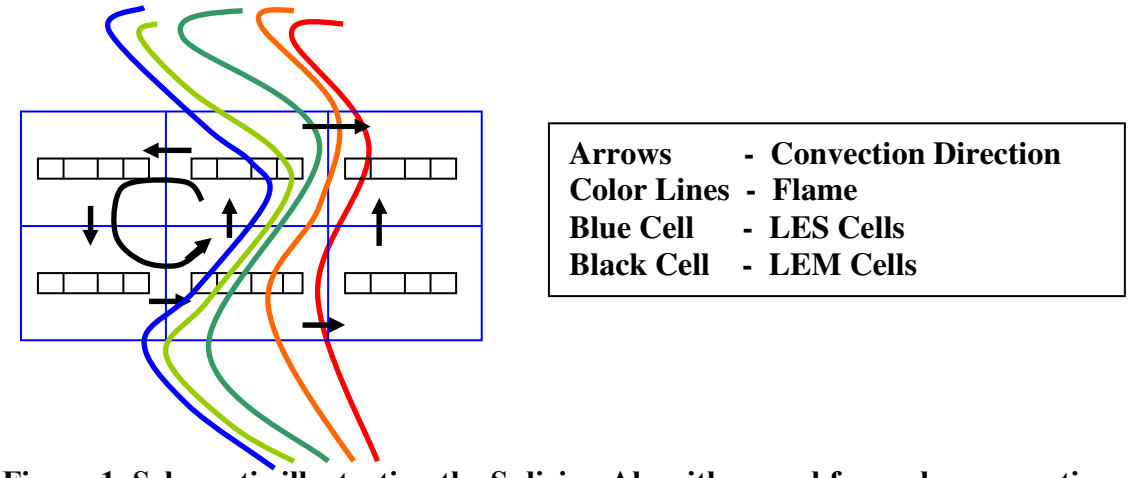


Figure 1. Schematic illustrating the Splicing Algorithm used for scalar convection.

3.5.1 New Splicing Algorithm Development under this Project

The earlier studies were limited to low-Mach number flows and therefore, some issues were substantially simplified and easy to implement. For example, in low-speed flows, the CFL time step is the convective time step, which is also the same time needed for the scalar transport via splicing. However, in the present study, we are eventually

interested in extending this approach to fully compressible flows, including supersonic flows. In this case, the CFL time-step is the acoustic time step whereas the scalar transport is still restricted by the convective time-step, which is at least an order of magnitude larger than the acoustic time-step. Thus, there is a possibility of de-coupling between the fluid dynamics (which evolves at the acoustic time) and the scalar transport (that occurs at the convective time). A substantial effort has been spent on understanding this issue and we have now developed a new convective transport model applicable for compressible flows.

The present splicing algorithm advects the sub-grid scalar field based on the mass, as opposed to the volume of the LEM cell that was used in the past. The advantage of using mass instead of volume is that, it ensures mass conservation at the resolved and unresolved scales at each instant of the calculation. Also in the earlier approach, partial LEM cells that have to be convected are accumulated, until they reach an integer value. In the new algorithm, every time a partial cell has to be convected out, a single cell of the same volume and mass, as that of the partial cell and with all the scalar properties is convected out. This potentially avoids the mass conservation errors and spurious numerical instabilities in the computation.

Volumetric expansion due to heat release and splicing by itself, also lead to a non-uniform distribution of the volume of the linear-eddy cells. To avoid programming complexities in a parallel environment, it is desirable to have same number of linear eddy cells everywhere in the computational domain. So, to equalize the volume of the linear-eddy cells and to retain the same number of linear eddy cells everywhere in the computational domain, the linear eddy domain is re-gridded to have cells of equal volume after each splicing. Errors introduced due to the spurious diffusion associated with re-gridding have not been evaluated yet. But it is expected to be minor, since at most only a couple of cells are affected.

Furthermore, to reduce any biasing error introduced by the operator splitting, the order in which reaction, diffusion and stirring are performed is switched after every splicing. An additional advantage of this switching is that, any discontinuities introduced by splicing are smoothed quickly by turbulent stirring, thus preventing any spurious diffusion.

3.5.2 Subgrid Simulation using LEM

The details of the sub-grid one-dimensional simulation using LEM are briefly summarized here. LEM is a stochastic model that treats reaction-diffusion and turbulent convection separately but concurrently. Reaction-diffusion processes evolve on a one-dimensional (1D) domain in which all the characteristic length scales in the turbulent field (from the integral scale L to the Kolmogorov η) are fully resolved (6 cells are used to resolve η). The orientation of the 1D domain is in the direction of the scalar gradient (and thus, for premixed flame, is in the flame normal direction), and within this domain, the equations governing constant pressure and adiabatic flame propagation are:

$$\frac{\partial Y_k}{\partial t} = -\frac{1}{\rho}\frac{\partial \rho Y_k V_k}{\partial x} + \frac{\dot{\omega}_k W_k}{\rho} + F_{kstir} \tag{8}$$

$$\frac{\partial T}{\partial t} = -\frac{1}{\rho \overline{C}_p}\sum_{k=1}^{N} C_{p,k} Y_k V_k \frac{\partial T}{\partial x} + \frac{1}{\rho \overline{C}_p}\frac{\partial}{\partial x}(\overline{\kappa}\frac{\partial T}{\partial x}) - \frac{1}{\rho \overline{C}_p}\sum_{k=1}^{N} h_k \dot{\omega}_k W_k + F_{Tstir} \qquad (9)$$

The equation of state for the scalar mixture is $P = \rho T \sum_{k=1}^{N} \frac{Y_k R_u}{W_k}$ and the caloric relation is given by $h_k = \Delta h^0_{f,k} + \int_{T0}^{T} C_{p,k}(T')dT'$. Here, T is the temperature, P is the thermodynamic pressure, R_u is the universal gas constant and ρ is the mass density. Also, $Y_k, W_k, C_{p,k}, \dot{\omega}_k, h_k, V_k$ and $\Delta h^0_{f,k}$ are respectively, mass fraction, molecular weight, specific heat at constant pressure, mass reaction rate, enthalpy, diffusion velocity and standard heat of formation (at standard temperature, T^o) of the *k*-th species. The mixture-averaged specific heat at constant pressure and thermal conductivity are respectively, $\overline{C}_p$ and $\overline{\kappa}$. Fickian diffusion velocity law: $V_k = -\frac{D_k}{Y_k}\frac{dY_k}{dx}$, where D_k is the mixture-averaged diffusivity of the *k*-th species, is used for molecular diffusion.

The convective terms $u_i \partial Y_k / \partial x_i$ and $u_i \partial T / \partial x_i$ in the species and the energy equations are represented as F_{kstir} and F_{Tstir}, respectively. These terms are implemented using stochastic re-arrangement events called triplet maps, each of which represents the action of a turbulent eddy on the scalar fields. It has been shown that this mapping can capture correctly the physical increase in scalar gradient (without affecting the mean scalar concentration) due to eddy motion. Three parameters are needed to implement these turbulent stirring events: the typical eddy size *l*, the eddy location within the 1D domain and the stirring frequency (event rate) λ. The eddy size in the range *L* to η is determined randomly from an eddy size distribution, *f(l)* which is obtained using inertial range scaling in three-dimensional turbulence: $f(l) = (5/3)\, l^{-8/3} / (\eta^{-5/3} - L^{-5/3})$. Here, η is determined from inertial range scaling law $\eta = N_\eta L\, Re^{-3/4}$ where N_η is an empirical constant. This constant reduces the effective range of scales between *L* and η but does not change the turbulent diffusivity, as described earlier.

The event location is randomly chosen from a uniform distribution and the event rate (frequency per unit length) is determined by:

$$\lambda = \frac{54}{5}\frac{\nu \mathrm{Re}}{C_\lambda L^3}\frac{[(L/\eta)^{5/3} - 1]}{[1 - (\eta/L)^{4/3}]} \qquad (10)$$

The time interval between events is then given as $\Delta t_{stir} = 1/(\lambda X_{LEM})$ where X_{LEM} is the length of the 1D domain.

The unique feature of the LEM model is that although the scalar evolution is simulated in 1D, the effect of turbulence on the scalar fields is modeled using 3D scaling laws. As a result, flame wrinkling occurs at spatial and temporal scales that mimics the effect of realistic 3D turbulent eddies on the flamelets. This formulation has two constants: C_λ and N_η both of which arise from the use of scaling laws. These parameters are obtained by comparing LEM predictions to experimental data in the flamelet regime (Smith and Menon, 1996). The present study uses these same values (C_λ = 15 and N_η = 4).

4. Progress to Date

Here, we summarize the progress made to date. It is worth noting that the project officially started at Georgia Tech in **late January 2002 and therefore, the progress noted below is for a period of 9 months**. We report here primarily on the effort carried out at Georgia Tech over this period. There were two major areas of progress: (a) transition of LES technology to NCC team at NASA/GRC and (b) further development of LES model for more complex flows.

4.1 Collaboration with NCC Team at NASA/GRC

Discussions with the NASA/GRC team members were carried out to set up the work plan. It was determined that one area that needs to be explored is the manner by which LES is carried out since it differs substantially from RANS application. It was also decided that this "learning" process needed to be carried out prior to implementing the LES routines into NCC. In order to do this Georgia Tech provided the NCC team with our advanced LES code, **LESLIE3D (Large-Eddy Simulations using Linear Eddy in 3D).** This code is the primary research tool employed at Georgia Tech to develop all the algorithms to be eventually implemented in NCC. Close collaboration has been established in order to "teach" the method for doing LES using our code.

4.1.1 LES Simulation strategy using LESLIE3D

In order to establish an understanding of how to do LES, the first phase of collaboration was to use the LESLIE3D to simulate a test case that has also been simulated at Georgia Tech. The NCC researchers have been using the LESLIE3D code to carry out the baseline simulation of the GE LM6000. This test case was also simulated at Georgia Tech and the detailed analysis package was also provided to NASA/GRC.

The test case is a full-scale GE LM6000 that was experimentally studied at GEAEC. Figure 2 shows the test configuration.

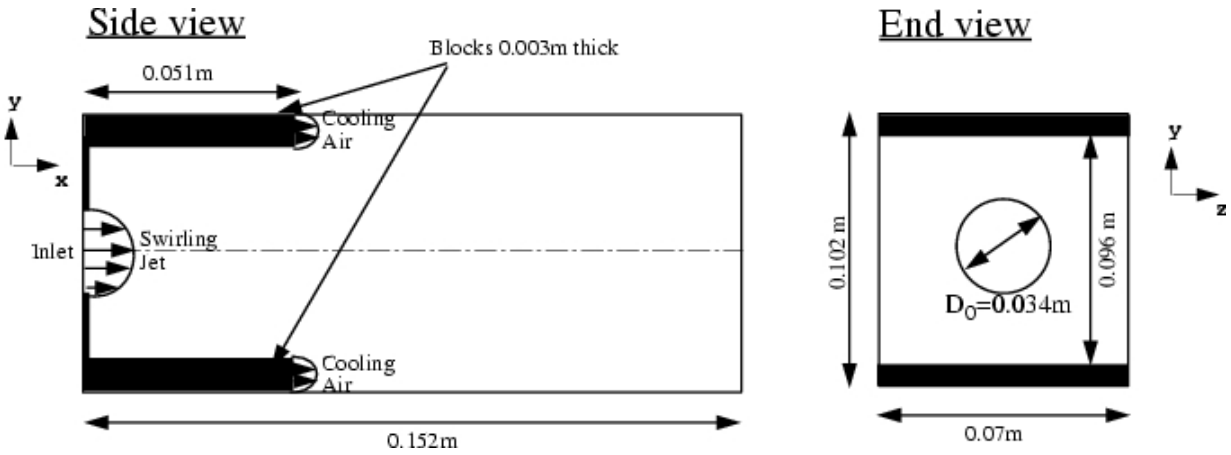


Figure 2. Schematic of the GE LM6000.

Premixed methane-air combustion is simulated under highly swirling conditions. The Reynolds number based on the inlet mean velocity and diameter is the 350,000, the inlet Swirl Number at the dump plane is 0.56, the inlet temperature is 688 Kelvin, the combustor mean pressure is approximately 6.5 ATM. We have employed relatively coarse grid of around 600,000 in the past to simulate this problem using the localized dynamic subgrid kinetic energy model and the dynamic flame speed model. A typical result is given in Fig. 3 which shows the centerline velocity decay. Various closure models for the subgrid diffusion term $G^{sgs} = (u_i G - \widetilde{u}_i \widetilde{G})$ were attempted but the results are relatively insensitive to them and all cases show reasonable agreement with data. Additional comparison of the velocity profiles also show good agreement.

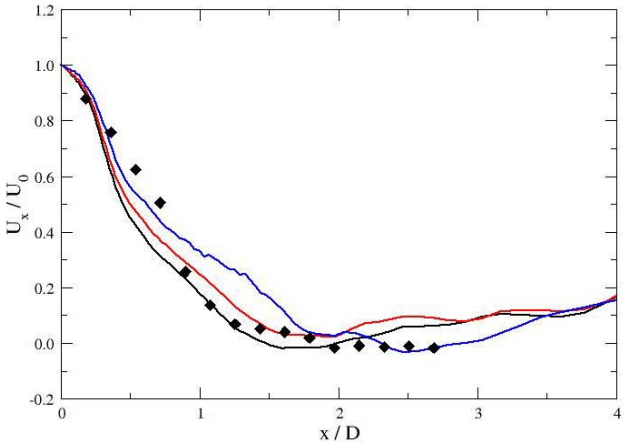


Figure 3. Centerline mean axial velocity variation. Symbols are the experimental data from GEAEC. The various lines correspond to the subgrid closure for the convective flux term $G^{sgs} = (u_i G - \widetilde{u}_i \widetilde{G})$. All models show reasonable agreement with data.

4.1.2 DNS of Decaying Isotropic Turbulence

Another area where collaboration has been established is in the area of inflow turbulence and initialization process. Typically, isotropic turbulence field is added to the mean flow. A version of the LESLIE3D was also developed and provided to NASA/GRC that can be used to generate isotropic turbulence. Since this solver has the ability to do both DNS and LES it was decided to simulate this sort of flow using both the second and fourth-order spatial schemes so that a baseline data base can be established to evaluate the ability of the NCC base scheme to simulate isotropic turbulence.

One case chosen for this purpose is direct numerical simulation (DNS) of decaying isotropic turbulence. Since the physics of the isotropic flows (such as the energy decay rate, form of the spectrum, etc.) are well established from the numerous experimental and numerical studies from the past, this exercise can serve as a powerful test-bed for establishing the capabilities of the code.

Decaying isotropic turbulent flow experiments of Comte-Bellot and Corrsin (CBC) (1971) were chosen for validating the compressible solver. In the experiments, measurements were taken at three locations downstream of the turbulence-generating grid. The mesh size of the grid was 5.08 cm and the mean velocity ahead of the grid was 10 m/s, giving a mesh Reynolds number of Re = 34000. Downstream of the grid, the wind tunnel had a slight contraction (1.27:1) that served to provide an isotropic condition. Conceptually, homogenous isotropic turbulence decays in time. However, in the wind tunnel environment, the turbulence decays in space as it evolves downstream. In order to convert a spatial evolution to the temporal evolution, Taylor's hypothesis is used and the turbulence in space is related to the decay in time of an imaginary box of homogenous turbulence through the relation: $t = \int_0^X \frac{dx}{\overline{U}(x)}$, where $\overline{U}(x)$ is the mean velocity of the flow at the streamwise location x.

To design a computation for the simulation of the CBC experiment, appropriate initial conditions that has the same spectrum as in the experiment is needed. In general the initial velocity field for the isotropic turbulence must satisfy at least three conditions: (a) conservation of mass, (b) the generated velocity field must be a real function of space and time, and (c) the turbulent field must have a realistic energy spectrum.

The first two conditions are required in order to obtain a stable numerical solution while the third conditions is needed to reduce the initial transient as the velocity field evolves to form realistic isotropic turbulence. In reality, not only does one need to specify the energy spectrum, but also the relative phases of the modes. In practice, however, this phase information is not available so that fields are usually constructed with random phase, but in such a way that they have a prescribed initial energy spectrum. Therefore, this initial condition will lead to a transient in which the phases adjust themselves to appropriate values.

The governing conservation equations for compressible flows are solved using a finite volume scheme that is second order in time and second or fourth order in space. In general, for a given Reynolds number, the second-order scheme requires twice the resolution of the fourth-order scheme to maintain DNS and/or LES accuracy. This is an important issue for model and code validation. The results reported below are for DNS and LES using the fourth-order scheme. The computational grid used is 64 x 64 x 64 with uniform spacing (for DNS) and periodic conditions are imposed on all the boundaries. The parameters corresponding to the simulation and the experiments are given in Table 1.

Table 1

Station	$\frac{\overline{U}t}{L}$	$\mathbf{Re}_\lambda$	Simulation	Grid
1	42	71.6	LES	32 x 32 x 32
2	98	65.3	DNS	64 x 64 x 64
3	171	60.3	DNS	64 x 64 x 64

The DNS simulations are initialized with a velocity field corresponding to the $\mathbf{Re}_\lambda$=65.3 (station 2, $\frac{\overline{U}t}{L}$=98) and is evolved for a time corresponding to the equivalent spatial distance between station 2 and station 3. Figure 4 shows the energy spectrum along with the experimental spectrum at two of the locations. It can be observed the present solver captures the energy cascade in the inertial range very well. The most significant aspect of this figure is that dissipation scales are resolved accurately. This is very important for any solver to demonstrate. If the numerical dissipation of the scheme is too high, dissipation range cannot be resolved very well. On the other hand, if the dissipation is not sufficient, the code becomes numerically unstable. The fact that the Kolmogorov cascade and the dissipation range of the spectrum are captured accurately is a proof that the code provides the correct amount of dissipation, while still retaining the stability of the solution. The deviation in the largest scales is because of the smaller size of the physical box used for the simulation. Since a bigger box size would require a higher resolution, slightly smaller box is used in the current simulation. But, as it is pointed out earlier, it is the smaller scales that are usually difficult to capture and hence, this should not be of any concern.

Figure 5 shows the vortical structures at the initial time and at a time when the turbulence has fully evolved. The decay of the turbulence and the growth of the small scales is clearly apparent in this figure.

4.1.3 LES of Decaying Isotropic Turbulence:

Having established the accuracy of the numerical scheme using the DNS, it remains to establish the accuracy of the sub-grid models employed in the present simulation. For this purpose, a large eddy simulation with a higher Taylor's Reynolds number ($\mathbf{Re}_\lambda$ = 71.6) was carried out. The initial velocity field was initialized with a velocity field that would provide the correct resolved and subgrid energy (as that in the experiments) corresponding to the computational grid (32 x 32 x 32) employed and the $\mathbf{Re}_\lambda$. A one-equation sub-grid kinetic energy along with an eddy-viscosity type closure is used to model the sub-grid scale processes. The rationale behind this and the validity of this approach has been very well established and documented.

Figure 6 shows the decay of the turbulent energy decay rate. As can be seen the current model accurately captures the energy decay rate from the large scales to the small scales. Sub-grid models are designed to provide dissipation from the resolved to the sub-grid scales and it is apparent that the current subgrid model provides the right amount of dissipation since otherwise it would not be possible to capture the correct decay rate

Figure 7 shows the energy spectrum from the present LES and the CBC experiment. Inertial range is captured very well despite the coarse grid used in the simulation. As expected, the energy spectrum deviates from the experiments at the small scales, since the dissipation range scales are not resolved explicitly in any LES. Finally, Figure 8 shows the evolution of the vorticity field from the current LES at the initial time and at a later time.

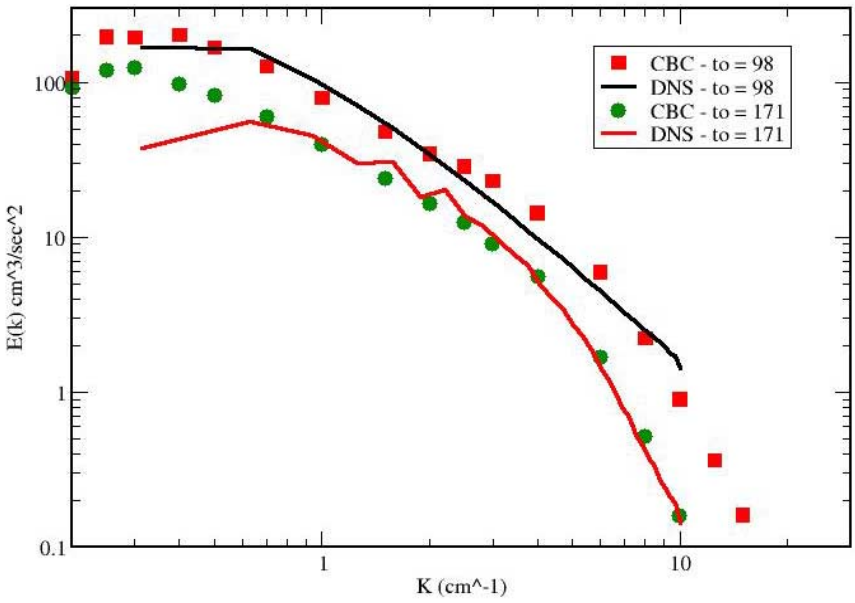


Figure 4. Energy Spectrum for Re_λ = 65.3 corresponding to CBC experiment.

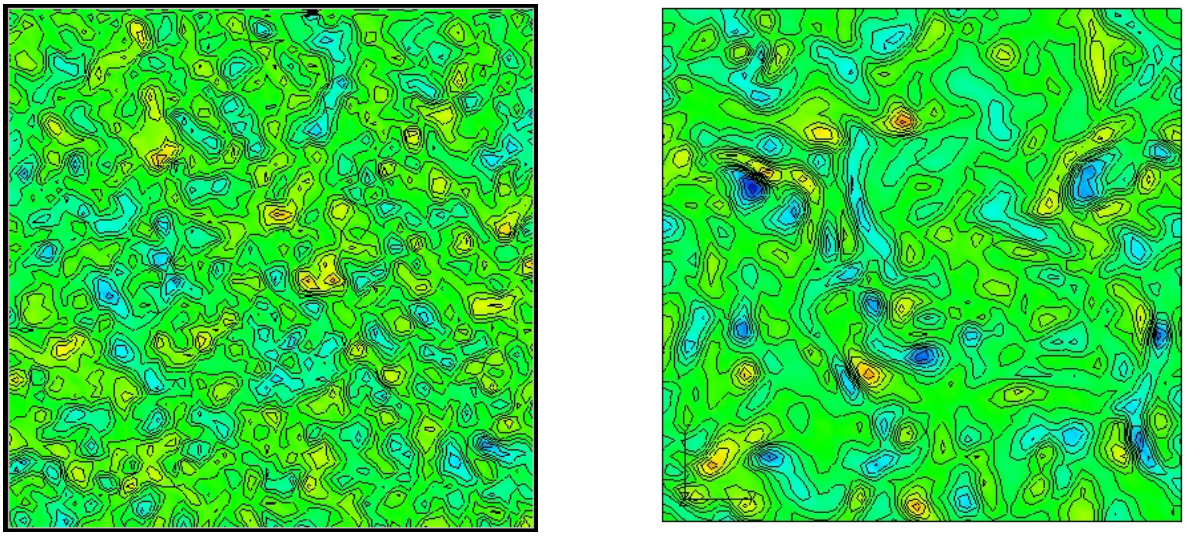


Figure 5. Vorticity Field corresponding to Re_λ = 65.3 at t = 0 and t = 0.2 seconds.

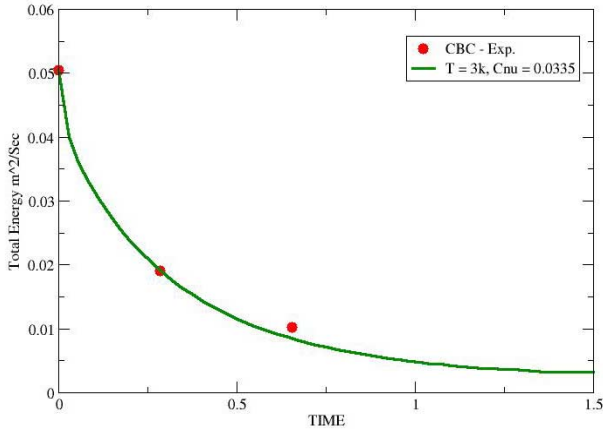


Figure 6. Kinetic Energy Decay in time.

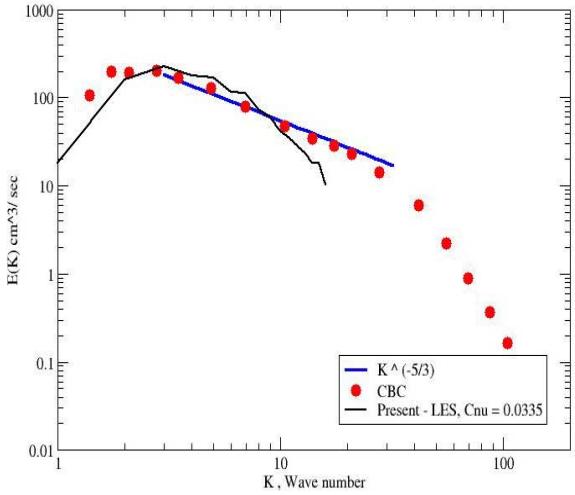


Figure 7. Turbulent Kinetic Energy spectrum for $Re_\lambda = 71.6$.

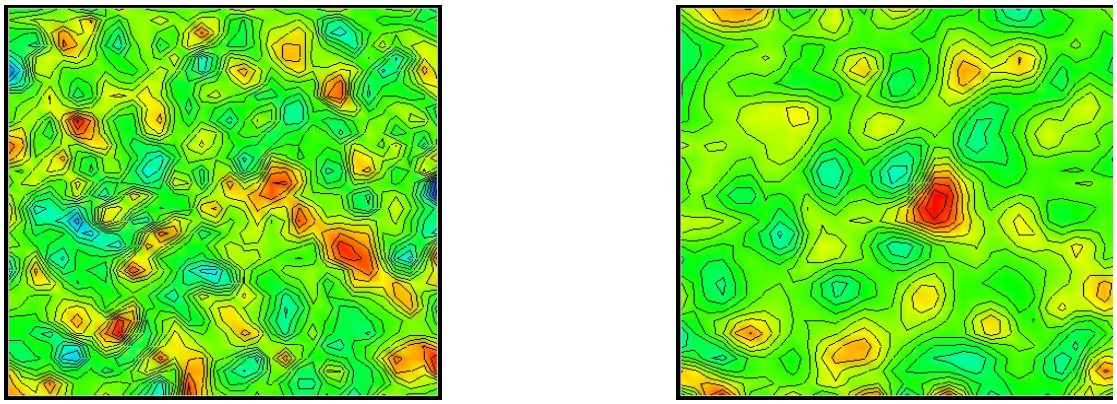


Figure 8. Vorticity Field in LES for $Re_\lambda = 71.6$ at initial time and at a later time.

4.2 Research Development at Georgia Tech

In addition to the collaboration with the NCC team reported in Section 4.1, research was undertaken at Georgia Tech to further develop the LESLIE3D code. Four areas have been under focus. These are (a) Flame-turbulence test problem for NCCLES validation, (b) LES of supersonic spatially evolving shear layers, (c) LES of combustion in the Trapped Vortex Combustor (TVC), and (d) DNS and LES of two-phase mixing layers. The reasons for the choice of these test cases are noted in the following sections.

4.2.1 Flame-Turbulence Test Problem for NCCLES Validation

The interaction of a premixed flame with turbulence is a well-established test problem used in many past studies to understand the impact of turbulence on flame dynamics. This problem is particularly suited for code validation since both DNS and LES have been carried out in the past (including detailed kinetics) and therefore, the physics of this problem is well established. This test case is also relatively simple to implement and test. This test problem can also be used for evaluating the algorithm's accuracy in reacting flows. Some results are reported below on the current effort.

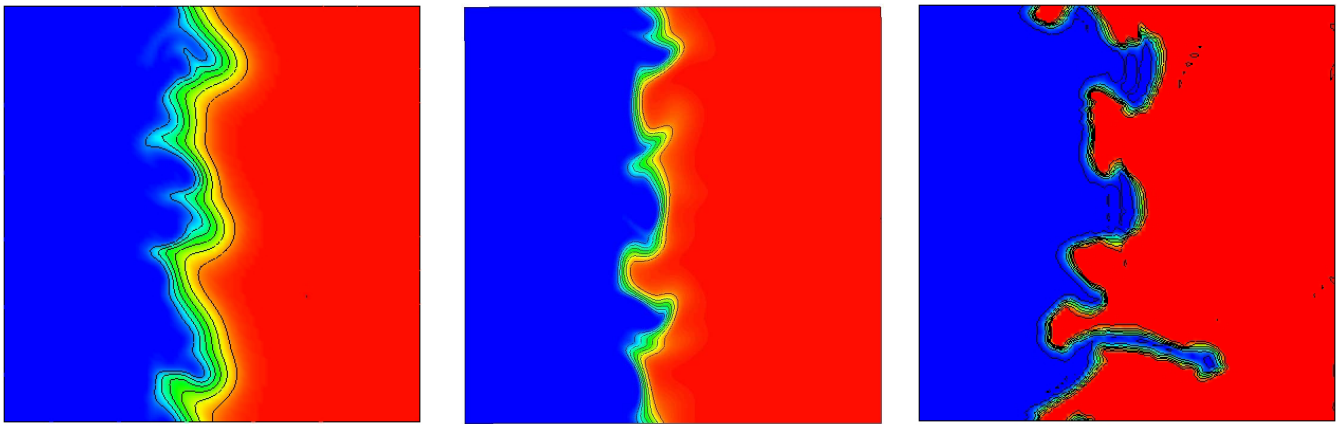
DNS and LES of the turbulent premixed stoichiometric methane-air flames with finite-rate effects have been performed. To reduce the cost of computations incurred due to the high resolution DNS and by the inclusion of finite rate chemistry, the simulations are restricted to two-dimensions. However, this is not a problem in this study since similar studies have been performed in the past (Echkeki and Chen, 1991) to understand flame-turbulence interactions.

The governing conservation equations are solved using a finite-volume scheme that is second-order accurate in time and fourth-order in space. The DNS was initialized in a two-dimensional computational domain with a plane laminar premixed flame. The reactant composition is a stoichiometric methane-air mixture at atmospheric pressure and temperature. The initialization for the scalars (species & Temperature) is obtained from a one-dimensional steady unstrained computations using PREMIX. A single step global chemistry (Westbrook and Dryer, 1971) with 5 species is used. The boundary conditions are periodic in the transverse direction and non-reflecting at the inflow and outflow (Poinsot and Lele, 1991). A computational grid of 400 x 400 with uniform spacing is employed for DNS and 100 x 100 for LES.

The initial turbulent field is generated from a specified energy spectrum, satisfying continuity. The spectrum is of the form: $$E(k) = 16u_o'^2 \frac{2}{\pi}\frac{k^4}{k_o^5}\exp\left\{-2\left(\frac{k}{k_o}\right)^2\right\},$$ where k is the wave number, k_o (= 6) is wave number of the most energy containing scale and u_o' is turbulent intensity which is equal to 10.57 m/s in the present simulation. The turbulence velocity field is super-imposed on the laminar flame. The ratio of the turbulence intensity u_o' to the laminar flame speed, S_L is 4.2 and the ratio of the integral scale to the laminar flame thickness, is 3.4. The turbulence Reynolds' number based on the integral scale is 137 and the Taylor's micro-scale is 36.

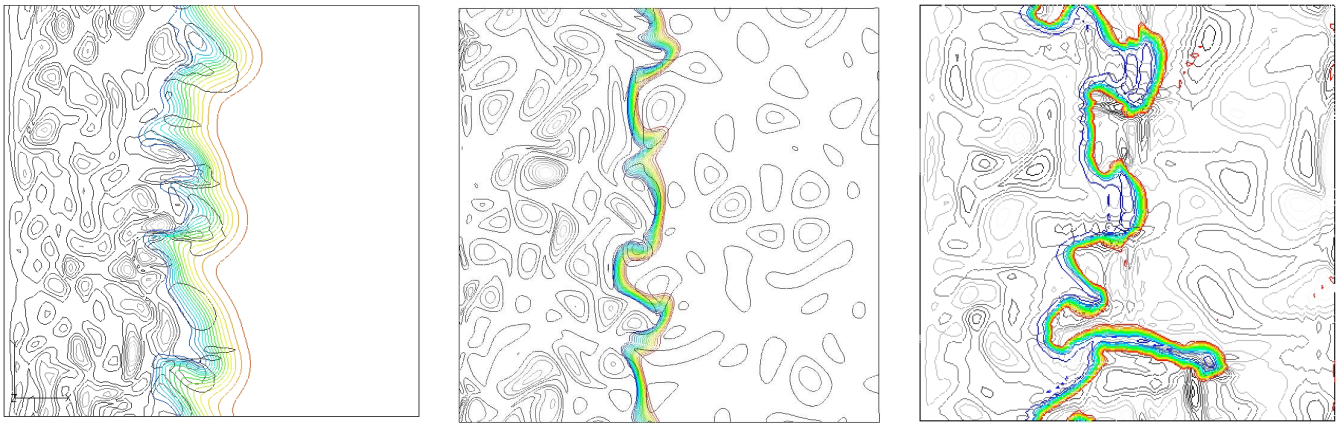
Three sets of simulations were carried out to contrast and compare the performance of the models employed in the present computations. DNS, LES-LEM and another LES using Eddy-Break-up closure (EBU) for scalars were performed. LES-LEM and LES-EBU simulations typically employed a uniformly spaced 100 X 100 computational grid. LES-LEM used 18 LEM cells per LES cell.

Figure 9 shows the instantaneous temperature contours computed using the LES-EBU, DNS and LES-LEM simulations, respectively. The flame topology indicates the presence of highly wrinkled flamelet due to flame-turbulence interactions. Note that LES-EBU diffuses the flame zone considerably, whereas LES-LEM actually makes the flame sharper when compared to the DNS. This is not surprising since LES-LEM actually captures the flame within the subgrid with very high resolution (actually better than DNS). For example, where as the DNS is capturing the flame over approximately 15 grid points, LES-LEM is capturing the flame over approximately 3-4 LES grid points. However, since there are 18 LEM cells per LES cell, the actual resolution is over 50 subgrid points. Thus, LES-LEM captures the flame very accurately. This is similar to what was observed earlier (Chakravarthy and Menon, 2001a, 2001b). This is demonstrated in Fig. 10 where the instantaneous vorticity and density contours for the three cases simulated are compared. (Contours not shown at the same time. Note, this is only a qualitative comparison). Vigorous interaction between the local vorticity and the flame are apparent from this figure.



(a) Eddy-Break-up (b) DNS (c) LES - LEM

Figure 9. Instantaneous temperature contours during flame-turbulence interaction. DNS is using 400x400 where as the LES is using 100x100. LES-LEM captures the flame as a sharp front (even better than DNS) since the subgrid resolution is better than in the conventional DNS. LES-EBU on the other hand diffuses the flame and fails to resolve the wrinkles.



(a) Eddy-Break-up (b) DNS (c) LES - LEM

Figure 10. Instantaneous density and vorticity contours during flame-turbulence interactions. Comparison is not shown at the same time. LES-LEM approach captures the flame very sharply compared to LES-EBU, even though same number of grid points are used in both the approaches,

4.2.2 LES of Supersonic Mixing Layers

One of the eventual goals of this project is to extend the NCCLES capability to supersonic combustion applications. However, in order to achieve this capability, the LES-LEM approach has to be extended to highly compressible flows.

The goal of the present study in the first year is to extend LES formulation to the highly compressible flows and to investigate the effects of the compressibility on the flows of engineering interest. In the first stage of this study the dynamic subgrid scale models are formulated with explicit correction terms, which accounts for compressibility effects. Simulations are underway for spatially evolving supersonic mixing layer for which there is some experimental data for model validation. Also, this particular flow was investigated earlier (Nelson and Menon, 1998) using an earlier version of the LESLIE3D code.

LES Equations for Compressible Turbulence:

The governing equations are obtained from Navier-Stokes equations by **using standard filtering instead of Favre filtering as done in the previous studies**. While it results in somewhat more complicated form of the governing equations than using Favre filtering, it provides for explicit terms that can be identified as “compressible” terms. Therefore, the modeling of these terms can be considered independently of the modeling issues typically used for the closure of the subgrid shear stresses.

The filtered LES equations can be written as

$$\frac{\partial \bar{\rho}}{\partial t} = -\frac{\partial \overline{\rho u_i}}{\partial x_i} - \frac{\partial}{\partial x_i}(\overline{\rho u_i} - \overline{\rho u_i}) \tag{11a}$$

$$\frac{\partial \overline{\rho u_i}}{\partial t} = -\frac{\partial \overline{\rho u_i u_j}}{\partial x_i} - \frac{\partial \bar{p}}{\partial x_i} + \frac{\partial \bar{t}_{ij}}{\partial x_{ij}} - \frac{\partial}{\partial x_j}(\overline{\rho u_i u_j} - \overline{\rho u_i u_j}) + \frac{\partial}{\partial x_j}(\bar{\tau}_{ij} - \bar{t}_{ij}) - \frac{\partial}{\partial t}(\overline{\rho u_i} - \overline{\rho u_i}) \tag{11b}$$

$$\frac{\partial \overline{\rho E}}{\partial t} = -\frac{\partial}{\partial x_i}(\overline{\rho E} + \bar{p})\bar{u}_i - \frac{\partial}{\partial x_i}(\overline{\rho u_i E} - \overline{\rho u_i E}) - \frac{\partial}{\partial x_i}(\overline{\rho u_i} - \overline{\rho u_i}) + \frac{\partial}{\partial x_i}(\overline{u_j t_{ij}}) +$$
$$+ \frac{\partial}{\partial x_i}(\overline{u_j \tau_{ij}} - \overline{u_j t_{ij}}) + \frac{\partial}{\partial x_i}(\bar{k}\frac{\partial \bar{T}}{\partial x_i}) + \frac{\partial}{\partial x_i}(\overline{k\frac{\partial T}{\partial x_i}} - \bar{k}\frac{\partial \bar{T}}{\partial x_i}) - \frac{R}{\gamma - 1}\frac{\partial}{\partial t}(\overline{\rho T} - \overline{\rho T}) -$$
$$- \frac{1}{2}\frac{\partial}{\partial t}(\overline{\rho u_i u_i} - \overline{\rho u_i u_i}) + \frac{\partial}{\partial t}(\bar{\rho} k^{sgs}) \tag{11c}$$

The resolved viscous stress tensor can be written as $\bar{t}_{ij} = 2\bar{\mu}(\frac{1}{2}(\frac{\partial \bar{u}_i}{\partial x_j} + \frac{\partial \bar{u}_j}{\partial x_i}) - \frac{1}{3}\frac{\partial \bar{u}_k}{\partial x_k}\delta_{ij}$

The total energy is $\bar{E} = \bar{e} + \frac{1}{2}\overline{u_i u_i} + k^{sgs}$, where subgrid kinetic energy is defined as $k^{sgs} = \frac{1}{2}(\overline{u_i u_i} - \overline{u_i u_i})$. The filtered equation of state $\bar{\rho} = \bar{\rho} R \bar{T} + R(\overline{\rho T} - \overline{\rho T})$ completes the set of the governing equations.

Compressibility correction terms:

The above LES equations contain additional terms that require closure. The density-velocity correlation terms in the continuity equation is purely a compressible term and this term is rewritten as the difference between Favre and conventionally filtered velocity: $c_i^{sgs} = \overline{\rho u_i} - \overline{\rho u_i} = \bar{\rho}(\tilde{u} - \bar{u})$. This term would vanish in the inviscid limit and it is generally negligible in the region of mild gradients (Chen et al., 1989). In the region of stronger gradients, it can be argued that the contribution of this term would be proportional to the mean density gradient, which lead to a gradient diffusion model for this term: $c_i^{sgs} = \overline{\rho u_i} - \overline{\rho u_i} \approx -\nu_c \frac{\partial \bar{\rho}}{\partial x_i}$ where ν_c is a "compressible viscosity'' that must be determined.

Since this term is expected to be significant only near strong density gradients, it is advantageous to formulate it in such a way that it would include a density gradient switch, avoiding therefore the excessive dissipation in the smooth mean flow regions. From dimensional consideration this term can be formulated as: $\nu_c = \alpha_c S_p \mid \overline{u_k} n_k \mid \Delta$ as "compressible viscosity correction term," where

$$\alpha_c = \begin{cases} \alpha_0 \exp\left(\dfrac{-1}{K_1(\mathrm{Re}_\Delta - \mathrm{Re}_{\min})}\right) & \mathrm{Re}_\Delta > \mathrm{Re}_{\min} \\ 0 & \mathrm{Re}_\Delta \le \mathrm{Re}_{\min} \end{cases} \tag{12}$$

Here, $\mathrm{Re}_\Delta = \dfrac{|\overline{u_k} n_k|\Delta}{\nu + \nu_t}$, where Δ the local grid spacing is the characteristic length scale and velocity normal to cell face is the velocity scale. The expression for the scaling coefficient α was obtained from the numerical simulations of 1-D non-linear Burger's equation (Nelson and Menon, 1998).

The turbulent eddy viscosity, used in the cell Reynolds number definition is defined as $\nu_t \approx c_\nu \sqrt{\overline{k^{sgs}}}\,\Delta$ (following Schumann, 1976) and used for modeling of 'incompressible' terms of subgrid scale closure equations.

The LES continuity equation can now be rewritten as

$$\frac{\partial \overline{\rho}}{\partial t} = -\frac{\partial \overline{\rho}\,\overline{u_i}}{\partial x_i} + \frac{\partial}{\partial x_i}\left(\nu_c \frac{\partial \overline{\rho}}{\partial x_i}\right) \tag{13}$$

The subgrid term in the momentum equation can be rewritten as $\tau_{ij}^{sgs(c)} = \overline{\rho u_i u_j} - \overline{\rho u_i}\,\overline{u_j}$. Again, as in continuity equation, compressibility effects are significant only near the regions of high gradients, and again the compressibility effects model should be triggered by the presence of high gradients (e.g., shocks). Since shocks were observed to have a dissipative effect on turbulence, the compressibility effect is modeled as an additional dissipation term $M_{ij}^{sgs(c)} \approx -2\overline{\rho}\nu_c\left(\overline{S_{ij}} - \frac{1}{3}\overline{S_{kk}}\delta_{ij}\right)$ where resolved rate of strain tensor is $\overline{S_{ij}} = \frac{1}{2}\left(\frac{\partial \overline{u_i}}{\partial x_j} + \frac{\partial \overline{u_j}}{\partial x_i}\right)$. Thus, the modeled momentum equation can then be written as

$$\frac{\partial \overline{\rho}\,\overline{u_i}}{\partial t} = -\frac{\partial \overline{\rho}\,\overline{u_i}\,\overline{u_j}}{\partial x_i} + \frac{\partial \overline{t_{ij}}}{\partial x_j} - \frac{\partial \overline{\rho}}{\partial x_i} - \frac{\partial \overline{\tau_{ij}^{sgs(i)}}}{\partial x_j} - \frac{\partial M_{ij}^{sgs(c)}}{\partial x_j} \tag{14}$$

The modeled subgrid kinetic energy equation in the compressible case is written as:

$$\frac{\partial \overline{\rho} k^{sgs}}{\partial t} = -\frac{\partial \overline{\rho} k_i^{sgs} \overline{u}_i}{\partial x_i} - \frac{\partial}{\partial x_i}\left(\overline{\rho}(\nu_t + \nu_c)\frac{\partial k^{sgs}}{\partial x_i}\right) - \tau_{ij}^{sgs}\frac{\partial \overline{u_j}}{\partial x_i} - \overline{\rho} c_\varepsilon \frac{(k^{sgs})^{\frac{3}{2}}}{\Delta} \tag{15}$$

This subgrid model contains two model coefficients which can be dynamically computed as before (Nelson and Menon, 1998). Finally, the compressibility effects in the energy subgrid model closure equation can be estimated as

$$\frac{\partial \overline{\rho}\,\overline{E}}{\partial t} = -\frac{\partial}{\partial x_i}(\overline{\rho}\,\overline{E} + \overline{\rho})\overline{u}_i + \frac{\partial}{\partial x_i}\left(c_e \overline{\rho}\sqrt{k^{sgs}}\,\Delta \frac{\partial \overline{H}}{\partial x_i}\right) + \frac{\partial}{\partial x_i}(\overline{u_j}\,\overline{t_{ij}}) + \frac{\partial}{\partial x_i}\left(\left(\overline{k} + \frac{\gamma c_v \overline{\rho}\nu_c}{\mathrm{Pr}}\right)\frac{\partial \overline{T}}{\partial x_i}\right) \tag{16}$$

This equation introduces yet another subgrid scale modeling coefficient, which can also be dynamically modeled as well.

Supersonic Spatial Mixing Layers: For validation of the numerical scheme and compressibility correction terms the comparison with Samimy et al (1991) experimental data was conducted. The original experiments were conducted in a high Reynolds number aerodynamic tunnel. Two stream mixing layers at different Mach numbers was separated at the entrance to the test region by a splitter plate. The flow scheme is provided in Figure 11. The optical test section IS 500x80 mm and velocity measurement were conducted using two-component laser Doppler velocimetry.

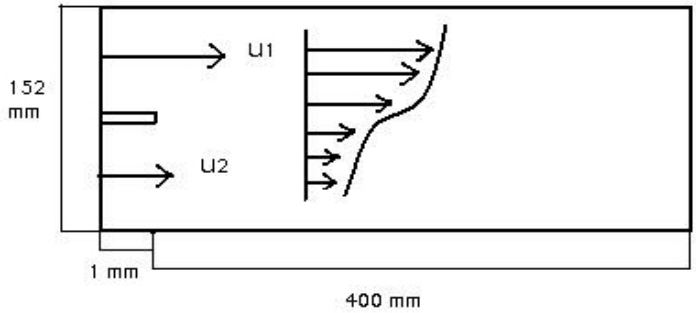


Figure 11. Spatially evolving supersonic mixing layer setup of Samimy et al. (1991).

The incoming flow parameters are provided in the Table 1.

T (K)	P_1 (kPa)	M_1	M_2	M_c	U_1 (m/s)	U_2/U_1	ρ_2/ρ_1	δ (mm)	Re
291.0	314.0	1.80	0.51	0.52	479.5	0.355	0.638	8.0	$9.4x10^6$

The computational area starts immediately after the edge of the splitter plate and has a length of 400mm and height 152 mm. Both upper and lower walls are slip walls. The periodic boundary is used in the z-direction. The inflow is fully specified on the supersonic part of the flow while on the subsonic part a characteristic boundary condition is used. The outflow boundary conditions are calculated using characteristic form of the governing equations using Poinsot and Lele method (1991). The initial conditions for the incoming boundary layers are computed using a 2-D boundary layer solver based on the known experimental data. For better comparison with the experiment a pseudo-turbulent velocity fluctuation are added to the inflow boundary. The turbulence with the assumed spectrum is calculated in a box and convected into the inflow boundary, scaled according to boundary layer solution on inflow boundary.

Figures 12 and 13 illustrates the instantaneous density, pressure and spanwise vorticity contours iso-surfaces for the developed mixing layer obtained in a recent simulation using the current LESLIE3D with the compressible correction. A grid 120x91x32 is employed for this simulation. This study is still underway and more results will be reported in the near future. Figure 14 shows the results obtained in an earlier study (Nelson and Menon, 1998), which compares the typical results for the shear growth rate and the normalized velocity profiles.

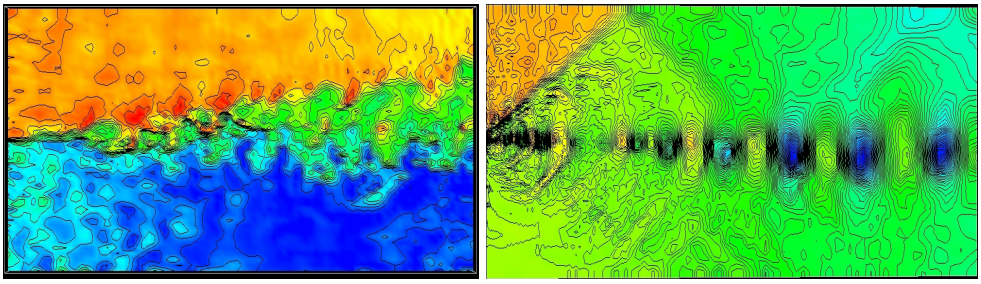


Figure 12. Iso-surfaces of density and pressure for the supersonic shear layer mixing.

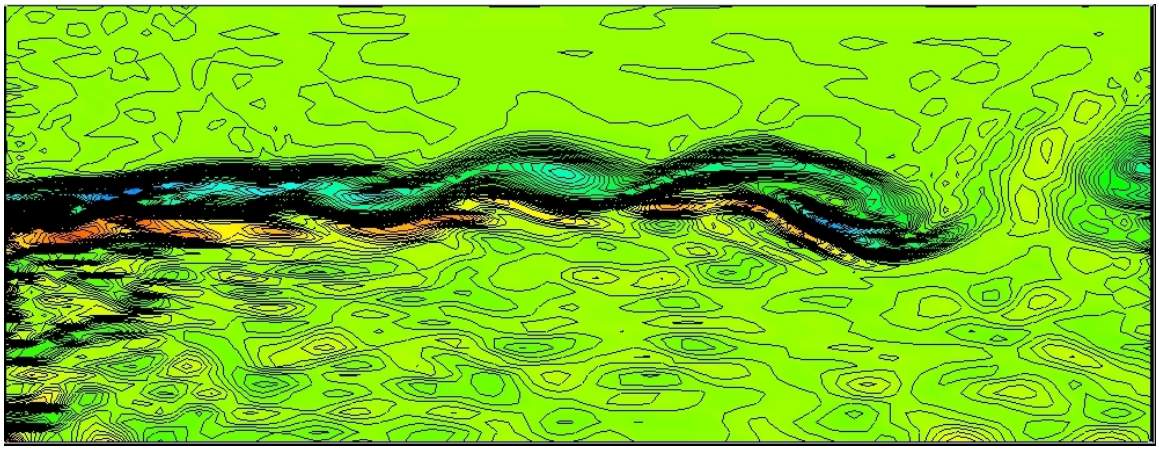


Figure 13. Spanwise vorticity in the supersonic shear layer.

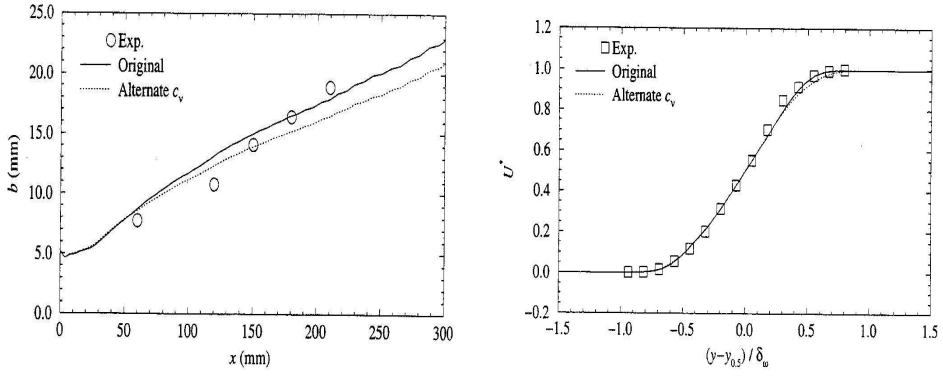


Figure 14. Comparison of the mixing layer growth and mean velocity profile with the experimental results. These results were obtained earlier (Nelson and Menon, 1998) but are being revisited for LESLIE3D validation in the supersonic regime.

The next step would be to attempt to compare the numerical simulation results with the DNS data for mixing layers with significant compressibility effects. This will be an area of research over the next few months.

4.2.4 DNS of Two-Phase Flows in Temporal Mixing Layers

Another area of research was in the development of DNS/LES methods for simulating single and two-phase mixing process in a temporal mixing layer. This test case is also chosen for NCCLES validation for some very important reasons:

(1) The current NCC code has the capability to do periodic conditions in only one-direction. Thus, with this capability, the isotropic turbulence test case noted in Section 3 will be quite difficult to accomplish unless major revision of the code is carried out. On the other hand, the temporal mixing layer can be simulated using periodic in one-direction and slip boundary conditions in the other two directions.
(2) The temporal mixing layer has been used extensively in the past for both DNS and LES studies and there is a large amount of data available for sort of flow. Also, temporal mixing layer is a subset mixing flow field of direct relevance to reacting flows.
(3) The gas phase temporal mixing layer simulation capability was developed many years ago at Georgia Tech. Here, we have extended its capability to simulate two-phase flows (e.g., spray mixing). This is with the focus for the eventual application to spray combustion, which is the major area of interest in the application of NCCLES.

In the following figures we show some samples of the DNS and LES studies using the temporal mixing layers. Results of the present DNS have been compared with DNS predictions in the past using a spectral code (Ling et al, 1998). Very good agreement with past studies is observed in all cases. The effect of particle size (as determined by the Stokes number) was the principal focus these studies. It can be seen that the simulations are able to capture all these effects accurately. The effect of using second-order and fourth-order spatially accurate schemes using the same grid resolution is also studied here. It can be seen that both schemes are reasonably accurate; however, the fourth-order scheme is better. In the present case, the second-order scheme is quite good since these simulations primarily focused on the rollup and pairing of large-scale coherent structures. These coherent structures are primarily 2D in their nature (and as initialized here) and therefore, the second-order scheme is reasonably accurate. However, if the mixing layer is initialized with 3D isotropic turbulence then it would become apparent that the fourth-order scheme would be superior for the same resolution.

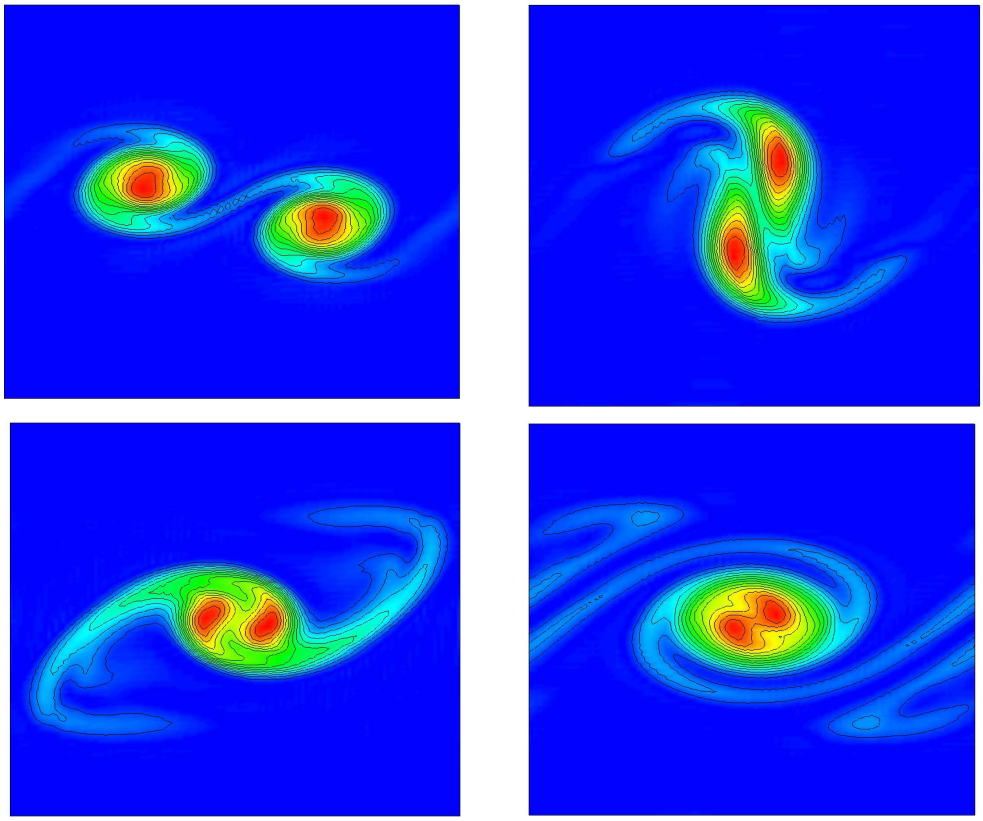


Figure 15. Evolution of the temporal mixing layer (shown here is the vorticity) during vortex pairing in the presence of particles for Stokes number of 4.

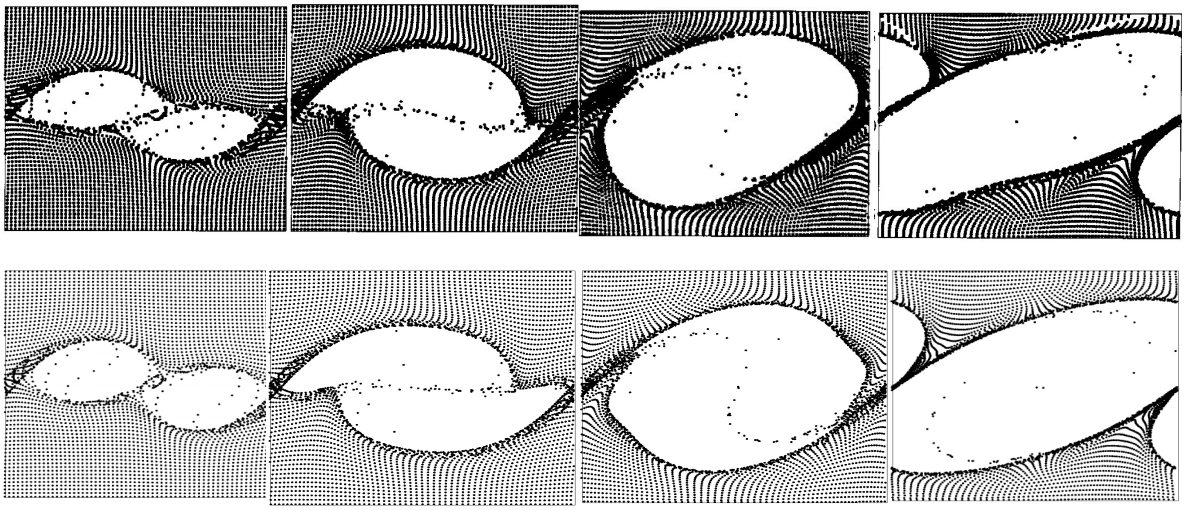


Figure 16. Particle motion and entrainment during vortex pairing (for a Stokes Number of 4). Top sequence is from DNS of Ling *et al* (1998) while the bottom sequence is from the present DNS study.

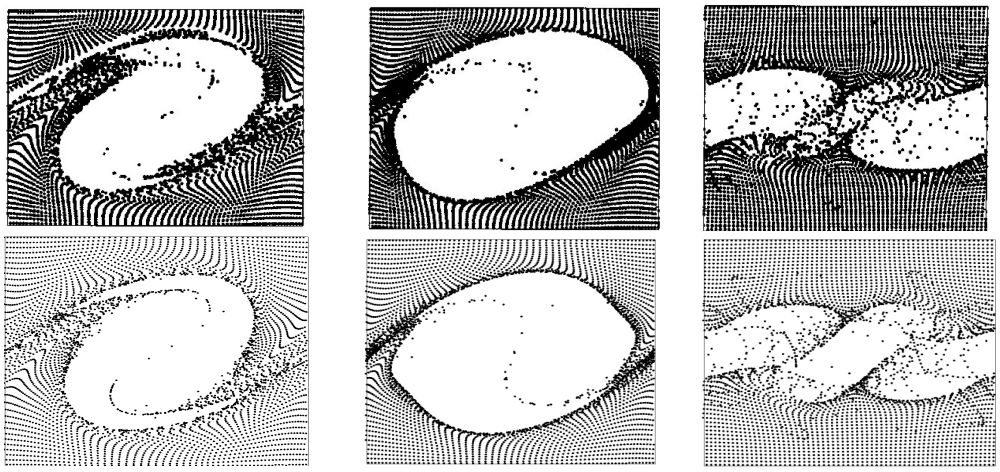


Figure 17. Comparison of past DNS (Ling et al, 1998 top series) prediction of particle motion with present DNS (bottom series) results. Figures from left to right are for Stokes Numbers of 1, 4 and 100, respectively at the same non-dimensional time.

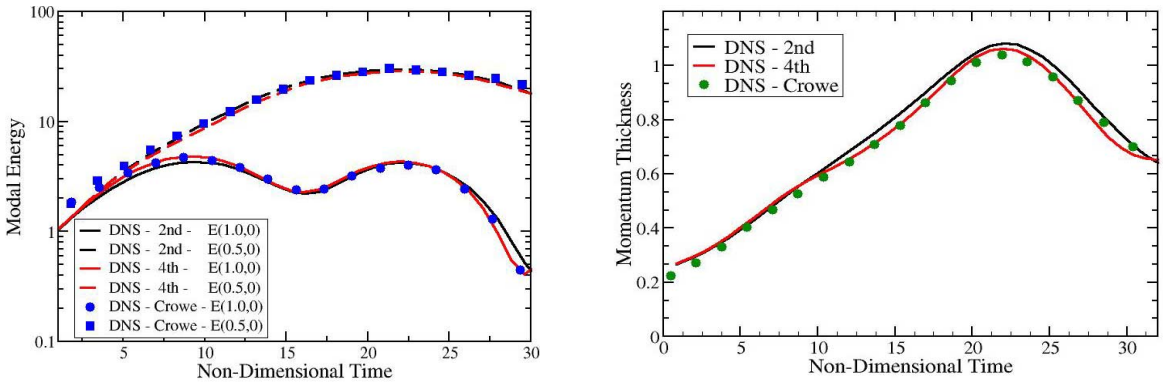


Figure 18. Modal energy and momentum thickness growth rates in the temporal mixing layer. The effect of second and fourth-order accuracy of the DNS is shown.

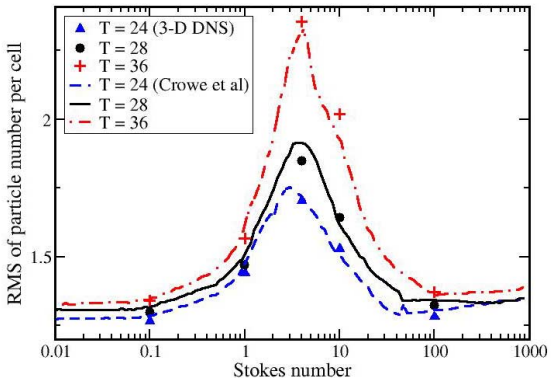


Figure 19. RMS of the particle number density in a cell as a function of Stokes Number is shown. Comparison with past DNS studies is shown.

5. Conclusions and Future Plans

The results reported here show that substantial progress has been made in the present research in this project. In addition to providing LESLIE3D codes and helping NASA/GRC researchers to understand LES methodology and its application, we have been developing additional features that will eventually find application in the NCCLES. In particular, three areas of development and validation are underway: (a) Flame-Turbulence Interactions using premixed combustion, (b) Spatially evolving supersonic mixing layers, and (c) Temporal single and two-phase mixing layers. The configurations chosen are such that they can be implemented in NCCLES and used to evaluate the ability of the new code.

The studies planned in the near future for the first year's effort is to complete the LES-LEM application in the flame-turbulence interactions and to further carry out LES of the supersonic spatially evolving shear layers. In addition, the extension of the LES-LEM approach for spray combustion will be addressed. In the second year, we anticipate further extension of the LES approach to more complex supersonic flows including shock waves.

In addition, in the second year we will begin LES study of the Trapped-Vortex Combustor (TVC). This combustor was chosen as a final test case for NCCLES and General Electric Aircraft Engine Company team had agreed to collaborate with the NASA/Tech team in this research. Therefore, we will begin discussion with GEAEC to identify a generic TVC configuration of their interest and begin setting up the LESLIE3D for this configuration. It is anticipated that some new insight into the TVC flow field will be achieved during the second years' effort under this project.

References

Ajmani, K. and K.-H. Chen (2001), "Unsteady-Flow Validation for the NCC," AIAA 2001-0972.

Bhargava, A., Kendrick, D.W., Colket, M.B., Sowa, W.A., Casleton, K.H., and Maloney, D.J. (2000), "Pressure effect on NOx and CO emission from industrial gas turbines," ASME, GT-97.

Chakravarthy, V.K. and Menon, S. (1997), "On Large-Eddy Simulations of Non-Homogeneous Flows," AIAA 97-0652, 35th Aerospace Sciences Meeting, Reno, NV, January 6-9, 1997.

Chakravarthy, V.K. and Menon, S. (2001a), "Modeling of Turbulent Premixed Flames in the Flamelet Regime," *Combustion, Science and Technology*, Vol. 162, pp. 1-50, 2001.

Chakravarthy, V.K. and Menon, S. (2001b) "Subgrid Modeling of Turbulent Premixed Flames in the Flamelet Regime," *Flow, Turbulence and Combustion*, Vol. 65.

Chen, C., Riley, J.J, and McMurthy, P.A. (1991) "A study of Favre averaging in turbulent flows with chemical reaction," *Combustion and Flame*, 87:257-277, 1991.

Calhoon, W. H. and Menon, S. (1997) "Linear Eddy Subgrid Modeling for Reacting Large-Eddy Simulations: Heat Release Effects," AIAA-97-0368, 35th Aerospace Sciences Meeting, Reno, NV, January 6-9, 1997.

Comte-Bellot, G., and Corrsin, S., Simple Eulerian time correlation of full- and narrow-band velocity signals in grid-generated, isotropic turbulence, *Journal of Fluid Mechanics*, 48:273-337, 1971.

Echekki, T., and Chen, J.H. (1991) "Unsteady Strain rate and curvature effects in turbulent premixed Methane-Air Flames," *Combustion and Flame*, 106:184-202, 1991.

Goldin, G. and Menon, S. (1997) "A Scalar PDF Construction Method for Steady State Turbulent Combustion," *Combustion Science and Technology*, Vol. 125, pp. 47-72, 1997.

Kee, R.J., Rupley, F.M., and Miller, J.A., Sandia National Laboratories report *SAND-8215b*, 1987.

Kim, W.-W. and Menon, S. (1998) "An Unsteady Incompressible Navier-Stokes Solvers for Large-Eddy Simulations of Turbulent Flows," *International Journal of Numerical Methods in Fluids,* Vol. 14, 1998.

Kim, W.-W. and Menon, S. (2000) "Numerical Modeling of Turbulent Premixed Flames in the Thin-Reaction-Zones Regime," Vol. 160, pp. 17-48, *Combustion Science and Technology*, 2000.

Kim, W.-W., Menon, S. and Mongia, H. (1999) "Numerical Simulations of Reacting Flows in a Gas Turbine Combustor," *Combustion Science and Technology*, Vol. 143, pp. 25-62, 1999.

Lannetti, A., R. Tacina, S.-M. Jeng, and J. Cai (2001) "Towards Accurate Prediction of Turbulent, Three-Dimensional Recirculating Flows with the NCC," AIAA-2001-0809.

Liu, N.-S. (2001) "On the Comprehensive Modeling and Simulation of Combustion Systems," AIAA-2001-0805, 38th Aerospace Sciences Meeting, Jan 2001.

Menon, S. (2000) "On Subgrid Modeling for Large-Eddy Simulations of Turbulent Combustion," *International Journal of Engine Research*, Vol. 1, No. 2., pp. 12-33.

Menon, S. and Calhoon, W. (1996) "Subgrid Mixing and Molecular Transport Modeling for Large-Eddy Simulations of Turbulent Reacting Flows," *Proceedings of the Combustion Institute*, 26, 59-66, 1996.

Menon, S., McMurtry, P., and Kerstein, A. R., "A Linear Eddy Mixing Model for LES of Turbulent Combustion," in Large-Eddy Simulations of Complex Engineering and Geophysical Flows, (B. Galperin and S. A. Orszag, Eds.), Cambridge University Press, pp. 287-314, 1993.

Menon, S., Yeung, P.-K. and Kim, W.-W. (1996) "The Effect of Subgrid Models on the Computed Interscale Energy Transfer in Isotropic Turbulence," *Computer and Fluids*, Vol. 25, pp. 165-186, 1996.

Moder, J. (2001) "Validation of the Radiation Heat Transfer Module Coupled with the Flow Solver in the NCC," AIAA-2001-0810.

Nelson, C. and Menon, S., "Unsteady Simulations of Compressible Spatial Mixing Layers," AIAA Paper No. 98-0786, 36th Aerospace Sciences Meeting, Reno, NV, January 12-15, 1998.

Pannala, S. and Menon, S., (1998) "Large-Eddy Simulations of Two-Phase Turbulent Flows," AIAA Paper No. 98-0163, 36th Aerospace Sciences Meeting, Reno, NV, January 12-15, 1998.

Poinsot, T., and Lele, S. (1991) "Boundary Conditions for Direct Simulations of Compressible Viscous Flow," *Journal of Computational Physics*, 101:1, 1991.

Raju, M. (2001) "A Validation Summary of Scalar Monte Carlo PDF Applied to Spray Flames," AIAA-2001-0806.

Samimy, M., Reeder, M.F., and Elliot, G. (1992) "Compressibility effects on large structures in free shear flows," *Physics of Fluids A*, 4(6):1251-1258, 1992.

Sankaran, V. and Menon, S. (2000) "The Structure of Premixed Flames in the thin-reaction zone," *Proceedings of the Combustion Institute*, Vol. 28, 2000.

Schumann, U. (1975) "Subgrid scale model for finite difference simulations of turbulent flows in plane channels and annuli," *Journal of Computational Physics*, 18:376-404, 1975.

Shih, T.-H., Norris, A., Lannetti, A. and Povinelli, L. (2001) "A Study of a Hydrogen/Air Combustor using NCC," AIAA-2001-0808.

Smith, T. and Menon, S. (1996) "Model Simulations of Freely Propagating Turbulent Premixed Flames," *Proceedings of the Combustion Institute*, 26, 299-306, 1996.

Sone, K. and Menon, S. (2001) "Large-Eddy Simulations of Fuel-air Mixing in Internal Combustion Engines," AIAA 2001-0910, Reno 2001.

Wei Ling, Chung, J.N., Troutt, T.R. and Crowe, C.T. (1998) "Direct numerical simulation of a three-dimensional temporal mixing layer with particle dispersion," *Journal of Fluid Mechanics*, 358:61-85, 1998.

Westbrook, C.K. and Dryer, F.L. (1981) "Simplified reaction mechanisms for the oxidation of hydrocarbon fuels in flames," *Combustion Science and Technology,* 27:31-43, 1981.

REPORT DOCUMENTATION PAGE

Form Approved
OMB No. 0704-0188

Public reporting burden for this collection of information is estimated to average 1 hour per response, including the time for reviewing instructions, searching existing data sources, gathering and maintaining the data needed, and completing and reviewing the collection of information. Send comments regarding this burden estimate or any other aspect of this collection of information, including suggestions for reducing this burden, to Washington Headquarters Services, Directorate for Information Operations and Reports, 1215 Jefferson Davis Highway, Suite 1204, Arlington, VA 22202-4302, and to the Office of Management and Budget, Paperwork Reduction Project (0704-0188), Washington, DC 20503.

1. AGENCY USE ONLY (*Leave blank*)	2. REPORT DATE	3. REPORT TYPE AND DATES COVERED
	April 2003	Final Contractor Report

4. TITLE AND SUBTITLE

Subgrid Combustion Modeling for the Next Generation National Combustion Code

5. FUNDING NUMBERS

WU–708–87–23–00
NAG3–2660

6. AUTHOR(S)

Suresh Menon, Vaidyanathan Sankaran, and Christopher Stone

7. PERFORMING ORGANIZATION NAME(S) AND ADDRESS(ES)

Georgia Institute of Technology
790 Atlantic Drive
Atlanta, Georgia 30332

8. PERFORMING ORGANIZATION REPORT NUMBER

E–13805

9. SPONSORING/MONITORING AGENCY NAME(S) AND ADDRESS(ES)

National Aeronautics and Space Administration
Washington, DC 20546–0001

10. SPONSORING/MONITORING AGENCY REPORT NUMBER

NASA CR—2003-212202
CCL–02–003

11. SUPPLEMENTARY NOTES

Project Manager, Nan Suey Liu, Turbomachinery and Propulsion Systems Division, NASA Glenn Research Center, organization code 5830, 216–433–8722.

12a. DISTRIBUTION/AVAILABILITY STATEMENT

Unclassified - Unlimited
Subject Categories: 01 and 07 Distribution: Nonstandard

Available electronically at http://gltrs.grc.nasa.gov

This publication is available from the NASA Center for AeroSpace Information, 301–621–0390.

12b. DISTRIBUTION CODE

13. ABSTRACT ***(Maximum 200 words)***

In the first year of this research, a subgrid turbulent mixing and combustion methodology developed earlier at Georgia Tech has been provided to researchers at NASA/GRC for incorporation into the next generation National Combustion Code (called NCCLES hereafter). A key feature of this approach is that scalar mixing and combustion processes are simulated within the LES grid using a stochastic 1D model. The subgrid simulation approach recovers locally molecular diffusion and reaction kinetics exactly without requiring closure and thus, provides an attractive feature to simulate complex, highly turbulent reacting flows of interest. Data acquisition algorithms and statistical analysis strategies and routines to analyze NCCLES results have also been provided to NASAJGRC. The overall goal of this research is to systematically develop and implement LES capability into the current NCC. For this purpose, issues regarding initialization and running LES are also addressed in the collaborative effort. In parallel to this technology transfer effort (that is continuously on going), research has also been underway at Georgia Tech to enhance the LES capability to tackle more complex flows. In particular, subgrid scalar mixing and combustion method has been evaluated in three distinctly different flow field in order to demonstrate its generality: (a) Flame-Turbulence Interactions using premixed combustion, (b) Spatially evolving supersonic mixing layers, and (c) Temporal single and two-phase mixing layers. The configurations chosen are such that they can be implemented in NCCLES and used to evaluate the ability of the new code. Future development and validation will be in spray combustion in gas turbine engine and supersonic scalar mixing.

14. SUBJECT TERMS	15. NUMBER OF PAGES
Subgrid mixing; Large eddy simulation; Spray combustion	35
	16. PRICE CODE

17. SECURITY CLASSIFICATION OF REPORT	18. SECURITY CLASSIFICATION OF THIS PAGE	19. SECURITY CLASSIFICATION OF ABSTRACT	20. LIMITATION OF ABSTRACT
Unclassified	Unclassified	Unclassified	